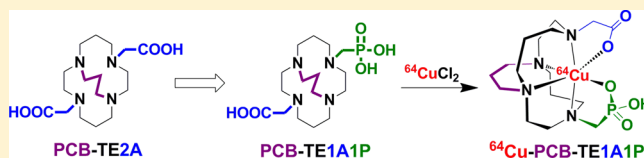


Synthesis and Evaluation of New Generation Cross-Bridged Bifunctional Chelator for  $^{64}\text{Cu}$  RadiotracersAjit V. Dale,<sup>†,‡</sup> Gwang Il An,<sup>‡,§</sup> Darpan N. Pandya,<sup>†</sup> Yeong Su Ha,<sup>†</sup> Nikunj Bhatt,<sup>†</sup> Nisarg Soni,<sup>†</sup> Hochun Lee,<sup>§</sup> Heesu Ahn,<sup>†</sup> Swarbhanu Sarkar,<sup>†</sup> Woonghee Lee,<sup>†</sup> Phuong Tu Huynh,<sup>†</sup> Jung Young Kim,<sup>‡</sup> Mi-Ri Gwon,<sup>||</sup> Sung Hong Kim,<sup>⊥</sup> Jae Gyu Park,<sup>⊗</sup> Young-Ran Yoon,<sup>||</sup> and Jeongsoo Yoo<sup>\*,†</sup><sup>†</sup>Department of Molecular Medicine, BK21 Plus KNU Biomedical Convergence Program, Kyungpook National University, Daegu 700-422, South Korea<sup>‡</sup>Molecular Imaging Research Center, Korea Institute of Radiological and Medical Sciences, Seoul 139-706, South Korea<sup>§</sup>Department of Energy Systems Engineering, Daegu Gyeongbuk Institute of Science & Technology, Daegu 711-873, South Korea<sup>||</sup>Department of Biomedical Science and Clinical Trial Center, BK21 PLUS, KNU Bio-Medical Convergence Program, Kyungpook National University Graduate School and Hospital, Daegu 700-422, South Korea<sup>⊥</sup>Analysis Research Division, Daegu Center, Korea Basic Science Institute, Daegu 702-701, South Korea<sup>⊗</sup>Pohang Center for Evaluation of Biomaterials, Pohang Technopark Foundation, Gyeongbuk 790-834, South Korea

## Supporting Information

**ABSTRACT:** Bifunctional chelators have been successfully used to construct  $^{64}\text{Cu}$ -labeled radiopharmaceuticals. Previously reported chelators with cross-bridged cyclam backbones have various essential features such as high stability of the copper(II) complex, high efficiency of radiolabeling at room temperature, and good biological inertness of the radiolabeled complex, along with rapid body clearance. Here, we report a new generation propylene-cross-bridged chelator with hybrid acetate/phosphonate pendant groups (PCB-TE1A1P) developed with the aim of combining these key properties in a single chelator. The PCB-TE1A1P was synthesized from cyclam with good overall yield. The Cu(II) complex of our chelator showed good robustness in kinetic stability evaluation experiments, such as acidic decomplexation and cyclic voltammetry studies. The Cu(II) complex of PCB-TE1A1P remained intact under highly acidic conditions (12 M HCl, 90 °C) for 8 d and showed quasi-reversible reduction/oxidation peaks at  $-0.77$  V in electrochemical studies. PCB-TE1A1P was successfully radiolabeled with  $^{64}\text{Cu}$  ions in an acetate buffer at 60 °C within 60 min. The electrophoresis study revealed that the  $^{64}\text{Cu}$ -PCB-TE1A1P complex has net negative charge in aqueous solution. The biodistribution and in vivo stability study profiles of  $^{64}\text{Cu}$ -PCB-TE1A1P indicated that the radioactive complex was stable under physiological conditions and cleared rapidly from the body. A whole body positron emission tomography (PET) imaging study further confirmed high in vivo stability and fast clearance of the complex in mouse models. In conclusion, PCB-TE1A1P has good potential as a bifunctional chelator for  $^{64}\text{Cu}$ -based radiopharmaceuticals, especially those involving peptides.



## INTRODUCTION

A rational approach to the design and synthesis of bifunctional chelators (BFCs) and systematic studies have resulted in great progress in metal-associated radiopharmaceuticals.<sup>1–4</sup> The increasing importance of Cu radioisotopes in medical imaging and radiation therapy is well-known.<sup>5–7</sup> In the design of radiopharmaceuticals involving Cu(II) metal ions, the BFC and target vector are important. The function of the BFC is to coordinate the radioactive Cu(II) ions with the help of inherently electron-donating atoms such as N and O, so that an appropriate chelation geometry is achieved. There are many literature reports on the essential qualities of BFCs for Cu(II)-based radiotracers.<sup>8–10</sup> Features such as high labeling at low temperatures (<40 °C), with fast kinetics, good in vitro and in vivo stabilities, and good clearance of the  $^{64}\text{Cu}$ -BFC complex are always necessary. Common and recently developed

macrocylic BFCs can be divided into three generations. DTPA,<sup>11</sup> DOTA,<sup>12</sup> TETA,<sup>13</sup> NOTA,<sup>14</sup> TE2A,<sup>15</sup> and their derivatives<sup>8,16</sup> (see Abbreviations for definitions of these materials) are classical BFCs containing N-acetic acid pendants. CB-TE2A,<sup>17</sup> PCB-TE2A,<sup>18</sup> and their analogues<sup>8,19</sup> are cross-bridged BFCs with N-acetic acid pendants. New generation cross-bridged BFCs, with N-acetic acid and N-phosphonic acid pendants, include CB-TE1A1P<sup>20</sup> and its modified forms (Figure 1).<sup>21</sup> Several BFCs have been reported, and each has its own benefits and shortcomings.

Since the early stages of the development of chelators for targeted Cu(II)-based radiopharmaceuticals, the focus has been on ease of construction of the chelator–biomolecule conjugate,

Received: December 8, 2014

Published: August 19, 2015

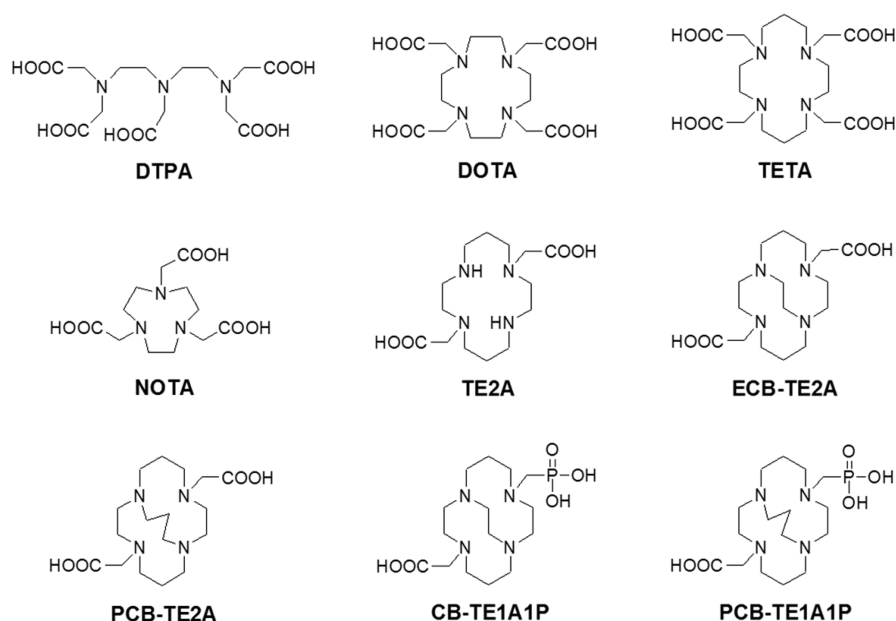
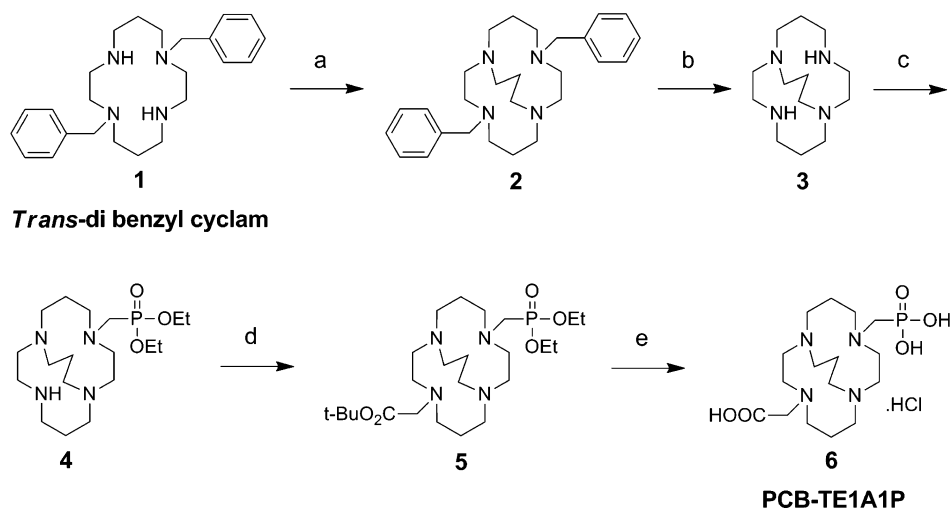


Figure 1. Various chelators developed for  $^{64}\text{Cu}$  radiolabeling.

Scheme 1. Synthesis Scheme of PCB-TE1A1P<sup>a</sup>



<sup>a</sup>(a) (i) 1,3-Propanediol di-*p*-tosylate,  $\text{K}_2\text{CO}_3$ , toluene, reflux 2 d, (ii) 20% NaOH, room temperature, 4 h, (69%), (b) 20%  $\text{Pd}(\text{OH})_2$ ,  $\text{CH}_3\text{COOH}$ , room temperature, overnight (99%), (c) paraformaldehyde,  $\text{P}(\text{OEt})_3$ ,  $\text{CHCl}_3$ , room temperature, 3–4 d, (60%), (d) *tert*-butyl bromoacetate,  $\text{K}_2\text{CO}_3$ ,  $\text{CHCl}_3$ , room temperature, 3–4 d, (90%), and (e) 6 M HCl, reflux, 10 h (70%).

labeling convenience, purification and isolation of the radio-tracer, and the ability to provide clear images, rather than on the radiometal–chelator–biomolecule stability.<sup>13,22–25</sup> However, the issue of the overall stability of the  $\text{Cu}(\text{II})$ -BFC complex was highlighted when it was reported that some conventional chelators lose  $^{64}\text{Cu}$  ions at an early stage in biological environments.<sup>26,27</sup> More attention has since been paid to the  $\text{Cu}(\text{II})$ -chelator stability. Among the developed chelators, CB-TE2A has proved to be an important BFC, because its  $\text{Cu}(\text{II})$  complex has good kinetic stability and in vivo inertness. However, a high temperature (90 °C) for more than 1 h is needed to achieve the ideal coordination geometry of the  $^{64}\text{Cu}$ -CB-TE2A radiocomplex; this limits its use as a BFC.<sup>17</sup>

In 2012, our group developed a new propylene-cross-bridged chelator, PCB-TE2A (Figure 1). The synthesis of this chelator

was convenient and simple. The  $^{\text{nat}}\text{Cu}/^{64}\text{Cu}$ -PCB-TE2A complex showed excellent stability in kinetic inertness studies and good in vivo properties in animal experiments. PCB-TE2A was quantitatively radiolabeled with  $^{64}\text{Cu}$  ions in a buffer solution at 70 °C.<sup>18</sup>

Recently, the group that initiated the use of CB-TE2A as a chelator for  $\text{Cu}(\text{II})$  radiopharmaceuticals reported a new ligand, CB-TE1A1P, containing acetic acid and phosphonic acid pendant arms. The design of CB-TE1A1P was based on the idea that the presence of phosphonic acid would enhance the  $\text{Cu}$  chelation kinetics, whereas the acetic acid pendant arm could be used for conjugation with biomolecules for targeting purposes. CB-TE1A1P shows good properties as a BFC; importantly, it can be radiolabeled with  $^{64}\text{Cu}$  ions at room temperature and has sufficient  $\text{Cu}$ -chelator stability.<sup>20</sup> This work triggered further structural modifications of CB-TE1A1P

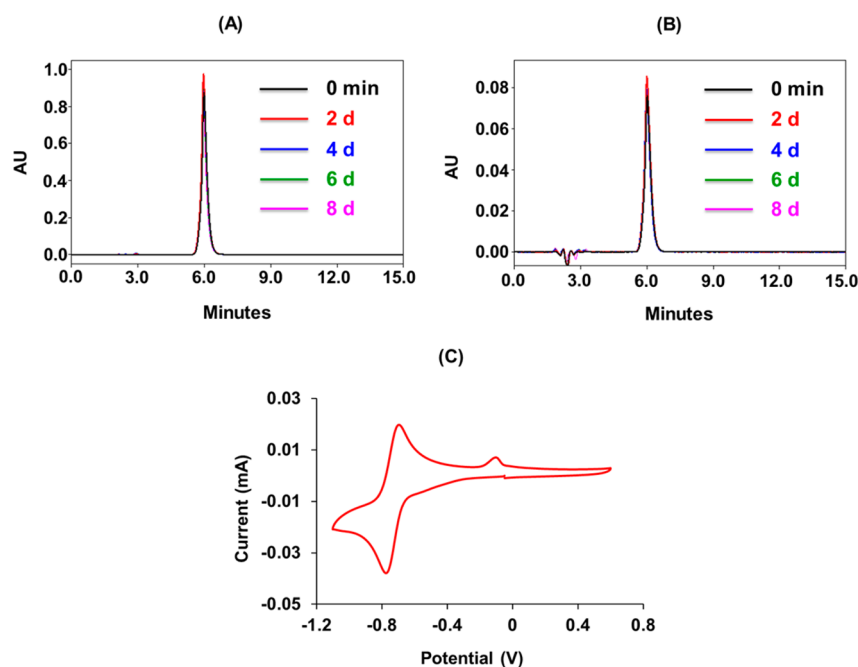


**Figure 2.** UV-HPLC chromatograms of Cu-PCB-TE1A1P at different times during acidic decomplexation study in 12 M HCl at 90 °C at (A) 280 nm and (B) 629 nm; (C) cyclic voltammogram (scanning rate 100 mV/s) of Cu-PCB-TE1A1P in PBS.

for the construction of more convenient Cu(II)-based radiopharmaceuticals.<sup>21</sup>

Attachment of a linker moiety to the chelator backbone for facile conjugation with biomolecules is the preferred method for the construction of Cu-carrying target-specific radiopharmaceuticals.<sup>5,19,21</sup> However, before this step, a thorough evaluation of the original linker-free chelator is necessary to determine whether the synthesized chelator meets the minimum requirements needed for a useful BFC. It has become common practice to assess the potential of newly synthesized chelators for use in future <sup>64</sup>Cu radio-tracers.<sup>15,18,20,28–30</sup>

A review of the relevant literature revealed that when one of the two acetic acid pendants in CB-TE2A was replaced by phosphonic acid, its radiolabeling profile improved significantly. In addition, the observation that PCB-TE2A was a favorable chelator for <sup>64</sup>Cu ions compared to CB-TE2A is important. We decided to determine the systematic changes when one of the acetic acid pendants of the PCB-TE2A chelator was replaced by a phosphonate group. In this work, we synthesized and studied a new chelator, PCB-TE1A1P, which features carboxylic acid and phosphonic acid pendants on the propylene-cross-bridged cyclam backbone (Figure 1). The reasoning behind the design of this chelator is that the structural similarities between PCB-TE1A1P and PCB-TE2A, that is, a propylene-cross-bridged cyclam and an acetic acid pendant, could significantly stabilize the Cu(II)-BFC complex, and the phosphonic acid pendant group could enable facile radiolabeling with <sup>64</sup>Cu ions at lower temperatures.

## RESULTS AND DISCUSSION

**Synthesis of Chelator PCB-TE1A1P.** The synthesis of a novel cross-bridged chelator, PCB-TE1A1P, was achieved in five steps, in 26% overall yield (Scheme 1). The starting material, *trans*-dibenzylcyclam **1**, was prepared using the reported method.<sup>31</sup> The propylene carbon chain was linked to the two *trans* secondary amino groups of **1** by refluxing with

1,3-propanediol di-*p*-tosylate in toluene using K<sub>2</sub>CO<sub>3</sub> as a base. This reaction first gave the tosylate salt of the *trans*-dibenzylpropylene cross-bridged cyclam **2**, and its free base was obtained by treatment with 20% NaOH. The catalytic hydrogenation of **2** yielded the important intermediate, that is, the propylene-cross-bridged cyclam **3**, which has two secondary amino groups at *trans* positions. The key step, namely, attachment of a single phosphonate pendant on only one of the two amine functionalities, was achieved by treating intermediate **3** with paraformaldehyde and triethyl phosphite at room temperature. As expected, an unwanted disubstituted phosphonate impurity was formed along with the desired product **4**. Good separation of the mono- and disubstituted products using thin-layer chromatography (TLC) enabled the pure propylene-cross-bridged cyclam with a monophosphonate pendant **4** to be obtained using column chromatography. This reaction condition gave monosubstituted **4** as the major product and the disubstituted byproduct as the minor one, when the starting material **3** was fully consumed. Initially, we tried to attach a *tert*-butyl acetate pendant to one of the secondary amine groups of compound **3**,<sup>20</sup> but the major product after consumption of **3** was the disubstituted product rather than the desired monosubstituted analogue. Addition of the *tert*-butyl acetate pendant on the remaining secondary amino group of intermediate **4** was performed at room temperature, by stirring **4** with *tert*-butyl bromoacetate and K<sub>2</sub>CO<sub>3</sub>, to yield PCB-TE1A1P precursor **5**. Finally, acidic hydrolysis of intermediate **5** under reflux conditions afforded the hydrochloride salt of the target chelator PCB-TE1A1P **6**.

**Synthesis of Cu-PCB-TE1A1P.** The Cu(II)-PCB-TE1A1P complex was obtained in 85% yield by refluxing an aqueous solution of PCB-TE1A1P and Cu(ClO<sub>4</sub>)<sub>2</sub>·6H<sub>2</sub>O for 10 min at a slightly basic pH (Scheme S1). The blue complex was purified using semiprep high-performance liquid chromatography (HPLC; Figure S1), and the analytical purity of the complex was confirmed using analytical HPLC (Figure S2). The Cu(II)-

PCB-TE1A1P complex displayed an absorption maximum ( $\lambda_{\text{max}}$ ) at 629 nm (5 M HCl, Figure S3).

#### Acidic Decomplexation and Electrochemical Studies.

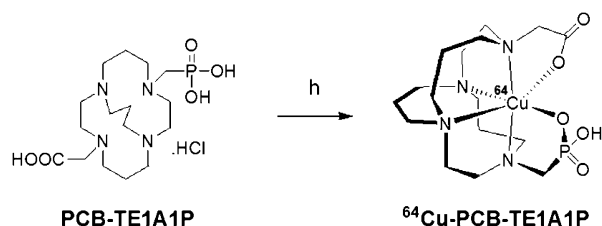
After synthesis of the Cu complex, the next step was to examine its kinetic stability. It has been reported that initial stability evaluation experiments on Cu(II) complexes, for example, acidic decomplexation and cyclic voltammetry studies, can help to anticipate their biological stability.<sup>32</sup> The experimental conditions for these stability studies are different from physiological conditions, but such experiments can be regarded as the first screening in monitoring the Cu–chelator stability. If the Cu–chelator complex displays poor stability in these initial studies, then radiolabeling studies of the BFC are unnecessary, because it has been observed that Cu(II)–BFC complexes that show low stabilities in these stability experiments are usually unstable in harsh physiological environments.<sup>32</sup> First, we monitored the stability of the Cu(II)-PCB-TE1A1P complex in 5 M HCl at 90 °C, using UV spectroscopy at 629 nm ( $\lambda_{\text{max}}$ ). The color and absorbance wavelength of the Cu complex did not change up to 2 d (Figure S4). This appreciable stability of Cu-PCB-TE1A1P inspired us to investigate acidic decomplexation using harsher conditions, that is, 12 M HCl and 90 °C. HPLC was used to monitor the reaction (Figure 2A,B). The Cu-PCB-TE1A1P complex remained intact in 12 M HCl at 90 °C for 8 d. Minimal changes in the color of the complex were observed even after 8 d in these acidic decomplexation studies. For comparison, Cu-PCB-TE2A could withstand these harsh conditions for 7 d, whereas Cu-CB-TE2A disintegrated completely within 8 h.<sup>18</sup>

We then performed cyclic voltammetry experiments to study the reduction/oxidation behavior of the Cu-PCB-TE1A1P complex. The results showed quasi-reversible reduction/oxidation peaks at  $-0.77$  V. A small hump at  $-0.1$  V (vs Ag/AgCl) was also seen; this could be attributed to oxidation of small amount of free Cu(I) ions to Cu(II) (Figure 2C). These data imply that even after reduction, most Cu(II)-PCB-TE1A1P complex holds Cu(I) ions in the tight chelation structure.

Analogous acidic decomplexation and cyclic voltammetry results were observed for Cu-PCB-TE2A, which displayed excellent stability, even better than that of Cu-CB-TE2A.<sup>18</sup> These results indicate that when one of the acetic acid pendants of PCB-TE2A was replaced by a phosphonate one, the stability of Cu(II)-PCB-TE2A was retained by the Cu(II)-PCB-TE1A1P complex. This high in vitro stability of Cu(II)-PCB-TE1A1P is one of the best yet reported for a Cu(II)-macrocyclic complex.<sup>18,20,32</sup>

**Radiolabeling of PCB-TE1A1P.** Our main purpose of synthesizing PCB-TE1A1P was to use it for  $^{64}\text{Cu}$ -labeling studies (Scheme 2). For this, we tried several conditions,

#### Scheme 2. $^{64}\text{Cu}$ Radiolabeling of PCB-TE1A1P<sup>a</sup>



<sup>a</sup>(h)  $^{64}\text{CuCl}_2$ , 0.1 M NaOAc (pH 8) buffer, 60 °C, 1 h (>95%).

including different buffers, chelator concentrations (0.1–100  $\mu\text{g}$ ), temperatures (50–90 °C), and reaction times (5–60 min). The radiochemical yield and purity were calculated using radio-HPLC (Figure 3, bottom) or radio-TLC (Figure S5). First, we

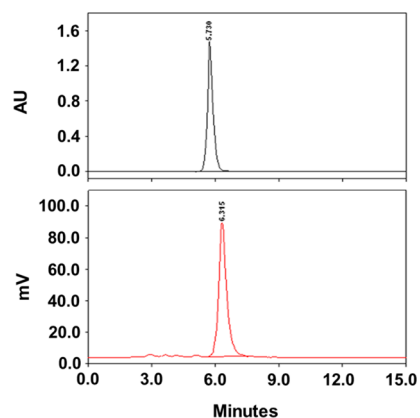


**Figure 3.** HPLC chromatograms of Cu-PCB-TE1A1P. (upper) UV-HPLC chromatogram of  $^{\text{nat}}\text{Cu}$ -PCB-TE1A1P (280 nm) and (lower) radio-HPLC chromatogram of  $^{64}\text{Cu}$ -PCB-TE1A1P.

determined the most suitable buffer and chelator concentration for  $^{64}\text{Cu}$ -PCB-TE1A1P labeling reactions. The NaOAc buffer gave higher radiolabeling yields (5–10%) than  $\text{NH}_4\text{OAc}$  buffer. Chelator amount of 1  $\mu\text{g}$  gave best labeling yield of >95% within 30 min using NaOAc buffer at 90 °C, whereas chelators of greater than 20  $\mu\text{g}$  or 0.1  $\mu\text{g}$  gave decreased radiolabeling yields of <90%. In further optimization of reaction time and temperature,  $^{64}\text{Cu}$ -labeling of PCB-TE1A1P was achieved in >95% radiochemical yield within 1 h by addition of  $^{64}\text{CuCl}_2$  to a solution of 1  $\mu\text{g}$  of chelator in 0.1 M NaOAc (pH 8) buffer at 60 °C (Table 1). As in the case of the nonradioactive Cu-PCB-

**Table 1.** Analysis of  $^{64}\text{Cu}$ -Radiolabeling Profile of PCB-TE1A1P in 0.1 M NaOAc (pH 8) Buffer Using 1  $\mu\text{g}$  of Chelator

| temperature (°C) | time (min) | radiolabeling yield (%) |
|------------------|------------|-------------------------|
| 50               | 60         | 40                      |
| 60               | 60         | >95                     |
| 70               | 30         | >95                     |
| 90               | 5          | 75                      |
| 90               | 10         | >95                     |

TE1A1P complexation reaction, complete labeling of PCB-TE1A1P with  $^{64}\text{Cu}$  ions was achieved within 10 min at 90 °C. But, the radiolabeling of  $^{64}\text{Cu}$ -PCB-TE1A1P at 50 °C gave only 40% yield within 1 h under the same conditions. We expected that the structural similarity of PCB-TE1A1P to CB-TE1A1P in terms of pendants and the cross-bridged-cyclam backbone might help  $^{64}\text{Cu}$ -radiolabeling of PCB-TE1A1P at room temperature. However, we have not yet achieved  $^{64}\text{Cu}$ -labeling of PCB-TE1A1P at temperatures below 50 °C. At present, it is difficult to comment further on radiolabeling assumptions and actual observations. However, it can be stated that the  $^{64}\text{Cu}$  radiolabeling profile of PCB-TE1A1P almost matched that of PCB-TE2A, with a minor improvement being seen in the case of PCB-TE1A1P.

**Determination of Partition Coefficient and Net Charge of  $^{64}\text{Cu}$ -PCB-TE1A1P.** Experiments to determine the partition coefficient were performed using the previously

reported 1-octanol/water method.<sup>33</sup> The  $\log(P)$  value of  $^{64}\text{Cu}$ -PCB-TE1A1P was  $-2.56$ , which indicates that  $^{64}\text{Cu}$ -PCB-TE1A1P is slightly less hydrophilic than  $^{64}\text{Cu}$ -PCB-TE2A having  $\log(P)$  value of  $-2.84 \pm 0.03$ .<sup>18</sup>

The overall net charge of  $^{64}\text{Cu}$ -PCB-TE1A1P was monitored using agarose gel electrophoresis (Figure 4).  $^{64}\text{Cu}$ -TETA,  $^{64}\text{Cu}$ -

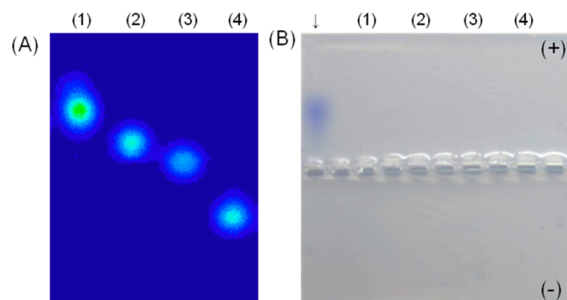


**Figure 4.** Agarose gel electrophoresis for measurement of net charge of  $^{64}\text{Cu}$  complexes. (A) Autoradiographic image and (B) photograph of the agarose gel. The complexes were loaded in following order: (1)  $^{64}\text{Cu}$ -TETA, (2)  $^{64}\text{Cu}$ -PCB-TE1A1P, (3)  $^{64}\text{Cu}$ -TE2A, (4)  $^{64}\text{Cu}$ -Cyclam. ↓ denotes loading dye.

TE2A, and  $^{64}\text{Cu}$ -cyclam were also run along with  $^{64}\text{Cu}$ -PCB-TE1A1P for direct comparison. As expected, the neutral complex  $^{64}\text{Cu}$ -TE2A did not move toward any side and stayed at the loading origin; however,  $^{64}\text{Cu}$ -TETA having overall net charge of  $-2$  moved toward the cathode, while  $^{64}\text{Cu}$ -cyclam having net charge of  $+2$  moved toward opposite direction, that is, the anode. The moving distance of  $^{64}\text{Cu}$ -TETA from the loading origin was almost the same as that of  $^{64}\text{Cu}$ -cyclam although the moving direction was opposite because both have the same magnitude of net charge of 2. However, in contrast to our expectation,  $^{64}\text{Cu}$ -PCB-TE1A1P moved toward cathode about two-fifths of the moving distance of  $^{64}\text{Cu}$ -TETA, suggesting that  $^{64}\text{Cu}$ -PCB-TE1A1P has almost overall net charge of  $-1$ . Considering its structural similarity with ethylene analogue  $^{64}\text{Cu}$ -CB-TE1A1P and X-ray structure of  $^{64}\text{Cu}$ -CB-TE1A1P having six coordination geometry including one oxygen coordination of phosphonate group,<sup>20</sup> it is reasonably anticipated that both acetate and phosphonate groups of PCB-TE1A1P also participate in Cu(II) complexation leading to overall neutral Cu(II) complex. Only explanation at current stage could be that noncoordinated  $-\text{OH}$  group of the coordinated phosphonate group may be deprotonated to render extra negative overall net charge to  $^{64}\text{Cu}$ -CB-TE1A1P in aqueous solution.

**In Vitro Stability Studies of  $^{64}\text{Cu}$ -PCB-TE1A1P.** The  $^{64}\text{Cu}$ -PCB-TE1A1P complex did not show any decomplexation up to 24 h in serum at  $37^\circ\text{C}$  (Figure S6).

The kinetic inertness of  $^{64}\text{Cu}$ -PCB-TE1A1P was monitored by measuring the rate of loss of  $^{64}\text{Cu}$  ion from the radiolabeled complex. The experimental procedure was slightly modified from the previous report.<sup>34</sup> In short, PCB-TE1A1P and DOTA were radiolabeled with  $^{64}\text{Cu}$  ions at  $90^\circ\text{C}$ , and the Cu(II) exchange experiment was performed at body temperature of  $37^\circ\text{C}$ . The labeled complexes were challenged with two different copper ion concentrations (1 and  $5\ \mu\text{M}$ ) in 5 mM HEPES buffer (pH 7.5). As summarized in Figure 5,  $^{64}\text{Cu}$ -PCB-TE1A1P did not show any loss of  $^{64}\text{Cu}$  ion from the labeled complex even at  $5\ \mu\text{M}$  of cold Cu(II) competition up to 3 h. In contrast,  $^{64}\text{Cu}$ -DOTA kept losing  $^{64}\text{Cu}$  from the complex in the

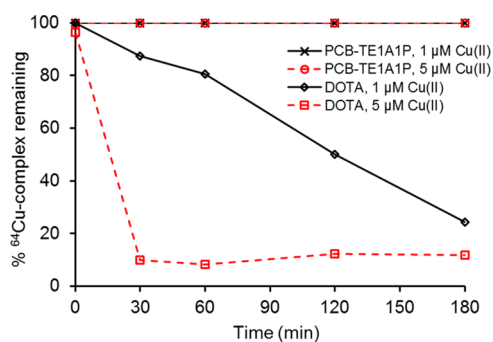


**Figure 5.** Percent of residual  $^{64}\text{Cu}$ -PCB-TE1A1P and  $^{64}\text{Cu}$ -DOTA as a function of incubation time at  $37^\circ\text{C}$  when challenged with nonradioactive  $\text{Cu}^{2+}$  (1 and  $5\ \mu\text{M}$ ) in HEPES buffer (pH 7.5).

presence of  $1\ \mu\text{M}$  of cold Cu(II) ion, and only 24% of intact  $^{64}\text{Cu}$ -DOTA was found at 3 h postincubation. In competition with  $5\ \mu\text{M}$  of cold Cu(II) ion, the 90% radioactive Cu(II) ions of  $^{64}\text{Cu}$ -DOTA were replaced with cold copper ions within 30 min. These copper(II) exchange experiments clearly indicate that PCB-TE1A1P forms much kinetically stable copper complex compared to commonly used DOTA.

**In Vivo Stability Study of  $^{64}\text{Cu}$ -PCB-TE1A1P.** In vivo stability experiments were conducted on  $^{64}\text{Cu}$ -PCB-TE1A1P using a modified version of a previously reported procedure.<sup>35</sup> HPLC analysis of intact  $^{64}\text{Cu}$ -PCB-TE1A1P and free  $^{64}\text{Cu}$  performed before rat injection showed a retention time of 5 and 3 min, respectively. In this blood analysis study, most  $^{64}\text{Cu}$ -PCB-TE1A1P was found to be intact in blood at 1 h postinjection (Figure 6); only small amount of free  $^{64}\text{Cu}$  ions

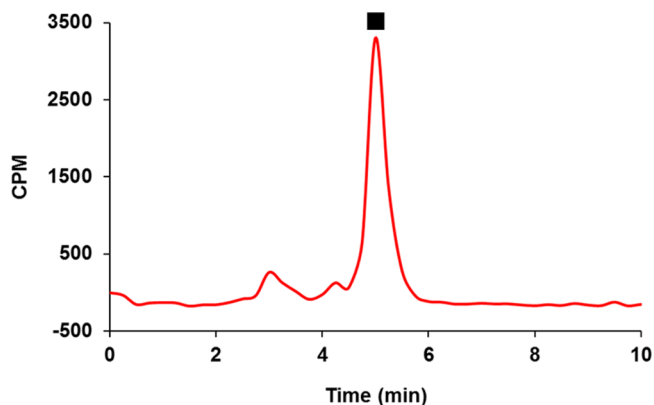


**Figure 6.** Radioactivity profile of processed blood of Sprague-Dawley rat injected with  $^{64}\text{Cu}$ -PCB-TE1A1P, showing intact  $^{64}\text{Cu}$ -PCB-TE1A1P (■).

are seen at 3 min. The presence of a high percentage of intact  $^{64}\text{Cu}$ -PCB-TE1A1P in blood of live animal strongly suggests its high stability in physiological condition, too.

**Biodistribution Studies.** After confirming the high in vitro and in vivo stability of  $^{64}\text{Cu}$ -PCB-TE1A1P, we performed biodistribution experiments using Sprague-Dawley rats to examine its body distribution and excretion patterns (Figure 7, Table S1). In general,  $^{64}\text{Cu}$ -PCB-TE1A1P displayed a rapid excretion profile. The kidney uptake of  $^{64}\text{Cu}$ -PCB-TE1A1P was maximum at 1 h ( $2.58 \pm 0.28\%$  ID/g). This kidney uptake decreased rapidly to  $1.11 \pm 0.14\%$  ID/g and  $0.40 \pm 0.02\%$  ID/g at 4 and 24 h postinjection, respectively. The liver uptake of  $^{64}\text{Cu}$ -PCB-TE1A1P was  $0.63 \pm 0.04\%$  ID/g at 1 h; this is less

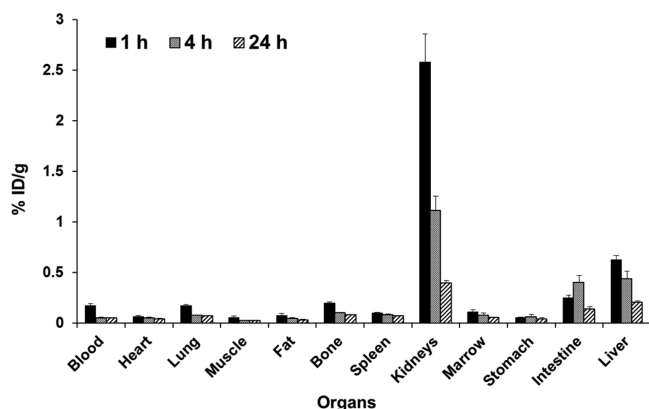


**Figure 7.** Biodistribution patterns of <sup>64</sup>Cu-PCB-TE1A1P at 1, 4, and 24 h postinjection in Sprague–Dawley rats ( $n = 5$ ).

than one-quarter of the kidney uptake in the same time period. This clearly indicates that <sup>64</sup>Cu-PCB-TE1A1P is preferentially cleared from the body via the urinary excretion system. The liver activity also showed progressive clearance with time ( $0.44 \pm 0.07$  and  $0.21 \pm 0.02\%$  ID/g at 4 and 24 h, respectively). Rapid clearance of <sup>64</sup>Cu-PCB-TE1A1P from the liver can be interpreted as a positive sign of high in vivo stability because dissociated free <sup>64</sup>Cu ions are rapidly trapped by liver proteins.<sup>20</sup>

Previously some phosphonate-containing radiotracers showed high bone uptake. When the radiocomplex cannot maintain the appropriate structural geometry, the phosphonate pendant does not coordinate to the radiometal and remains free in a biological environment. This type of unbound phosphonate functional group has an affinity with bone. High bone uptake can therefore be an indication of lower complex stability.<sup>36–41</sup> Here, <sup>64</sup>Cu-PCB-TE1A1P showed little bone uptake from the initial time point ( $0.20 \pm 0.01\%$  ID/g at 1 h) and decreased to  $0.10 \pm 0.002\%$  ID/g at 4 h and  $0.08 \pm 0.004\%$  ID/g at 24 h. These results indicate that the radiotracer does not target bone and retains the appropriate complex geometry. Very minimal <sup>64</sup>Cu-PCB-TE1A1P radioactivity was observed in the remaining nonclearance organs at 24 h ( $<0.08\%$  ID/g). These biodistribution data suggest that the <sup>64</sup>Cu-PCB-TE1A1P complex has rapid clearance properties with the least transchelation of <sup>64</sup>Cu ions from the chelator to biomolecules.<sup>26,27,42</sup>

#### Positron Emission Tomography Imaging Study.

Whole-body positron emission tomography (PET) images of <sup>64</sup>Cu-PCB-TE1A1P in normal BALB/c mouse are displayed in Figure 8. As seen in biodistribution data, the activity cleared fast from the body mainly via the urinary track. At 1 h postinjection, the hottest activities were seen in the kidneys ( $5.60 \pm 0.14\%$  ID/g) and bladder. The liver ( $2.85 \pm 0.07\%$  ID/g) also showed high activity accumulation next to the kidneys. At 4 h, most activities (>90% of injected activity) already cleared from the body. The kidneys ( $1.95 \pm 0.07\%$  ID/g) still showed higher activity than the liver ( $1.30 \pm 0.14\%$  ID/g). More concentrated activities were found in the bladder and intestine. At 24 h, any noticeable uptakes were seen in background except abdominal region and feces. The remaining activities in the liver and kidneys are less than 0.4% ID/g. Any noticeable uptake in bone was not detected in PET/CT fusion image (Figure 8D), which strongly suggests that the phosphonate group of PCB-TE1A1P makes coordination bond to Cu(II) atom but does not exist free as a bone seeking moiety.

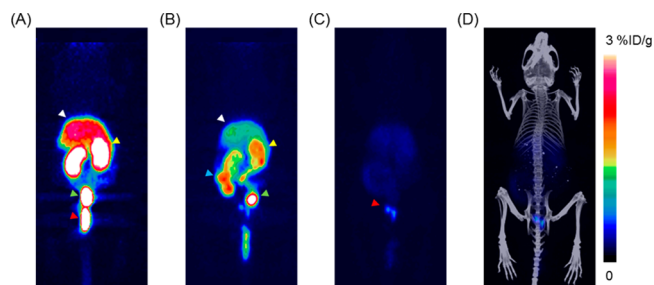


**Figure 8.** PET maximum intensity projection image of <sup>64</sup>Cu-PCB-TE1A1P at (A) 1, (B) 4, and (C) 24 h postinjection of <sup>64</sup>Cu-PCB-TE1A1P in normal BALB/c mouse. (D) PET/CT fusion image at 24 h postinjection. White arrowhead, liver; yellow arrowhead, kidney; green arrowhead, bladder; red arrowhead, feces; skyblue arrowhead, intestine.

## CONCLUSION

In conclusion, we have successfully synthesized a new chelator, PCB-TE1A1P, which contains carboxylic and phosphonic acid pendants on a propylene-cross-bridged tetraazamacrocyclic backbone. The structural similarity between PCB-TE1A1P and PCB-TE2A provides substantial kinetic stability to the Cu(II)-PCB-TE1A1P complex. PCB-TE1A1P was radiolabeled with <sup>64</sup>Cu ions in a simple buffer solution at 60 °C. The results of biological experiments clearly show that <sup>64</sup>Cu-PCB-TE1A1P has good stability and rapid clearance in physiological environments. All these features make PCB-TE1A1P a promising BFC for future research on <sup>64</sup>Cu radiotracers. Although PCB-TE1A1P was not radiolabeled at room temperature, it could still be used for the preparation of <sup>64</sup>Cu-based radiopharmaceuticals involving peptides. This objective could be achieved either by conjugating the carboxylic acid pendant of PCB-TE1A1P with the primary amino groups of peptides<sup>43</sup> or modifying the chelator structure with additional linkers on propylene cross-linker.<sup>19</sup>

## EXPERIMENTAL SECTION

**General.** All reagents and solvents were purchased from Sigma-Aldrich (St. Louis, MO, USA) and were used as received. Copper-64 was produced at KIRAMS (Seoul, Korea) via the <sup>64</sup>Ni(p,n)<sup>64</sup>Cu nuclear reaction using an MC50 cyclotron (Scanditronix, Sweden). All <sup>1</sup>H NMR and <sup>13</sup>C NMR spectra were measured on Varian Unity Inova400 and 500 MHz instrument. High-resolution mass spectra (HRMS) were recorded on JEOL JMS700 or Quattro Premier XE mass spectrometer. UV–vis spectra were acquired on a Shimadzu UV–vis spectrophotometer (UV-1650PC). HPLC traces were acquired using Waters 600 series HPLC system. The radio-TLC measurements were performed using a Bioscan 2000 imaging scanner (Bioscan, Washington, DC, USA).

**Synthesis of 4,11-N,N'-Bis(benzyl)-1,4,8,11-tetraazabicyclo-[6.6.3]heptadecane (2).** *trans*-Dibenzylcyclam **1** (3.56 g, 9.35 mmol), 1,3-propanediol di-*p*-tosylate (4.67 g, 12.16 mmol), and anhydrous K<sub>2</sub>CO<sub>3</sub> (6.46 g, 46.75 mmol) in anhydrous toluene (200 mL) were placed in a 500 mL round-bottomed flask. The reaction mixture was refluxed for 2 d; a calcium chloride guard tube was placed on top of the condenser to exclude moisture. Completion of the reaction was determined using TLC. The resulting reddish-brown reaction mixture was filtered through a pad of diatomaceous earth and washed with sufficient CH<sub>2</sub>Cl<sub>2</sub>. The solvent was evaporated under reduced pressure using a rotary evaporator; the tosylate salt was obtained as a brownish sticky mass. This salt was dissolved in 20% NaOH (200 mL) solution, and the mixture was stirred for 6 h. The reaction mixture was extracted with CH<sub>2</sub>Cl<sub>2</sub> (3 × 75 mL); the CH<sub>2</sub>Cl<sub>2</sub> layers were washed with brine and dried over MgSO<sub>4</sub>. The solvent was

evaporated under reduced pressure using a rotary evaporator. The resulting residue was subjected to column chromatography with silica gel as the stationary phase and  $\text{CH}_2\text{Cl}_2/\text{MeOH}$  (10:1.5) as the eluent, to afford off-white solid **2** (2.71 g, 69% yield). TLC conditions: silica gel,  $\text{CH}_2\text{Cl}_2/\text{MeOH}$  10:1.5, Dragendorff's reagent,  $R_f$  value: 0.5–0.6. Spectroscopic data:  $^1\text{H}$  NMR (500 MHz,  $\text{CDCl}_3$ ):  $\delta$  7.26–7.14 (m, 10H), 3.68–3.65 (d, 2H,  $J = 14$  Hz), 3.52–3.49 (d, 2H,  $J = 14$  Hz), 3.08–2.51 (m, 20H), 1.80 (brs, 4H), 1.60–1.26 (m, 2H);  $^{13}\text{C}$  NMR (125 MHz,  $\text{CDCl}_3$ ):  $\delta$  135.8, 129.8, 128.3, 127.4, 58.8, 56.6, 54.2, 52.8, 47.4, 22.6, 19.9; high-resolution mass spectrometry fast atom bombardment (HR-MS FAB) calculated for  $\text{C}_{27}\text{H}_{41}\text{N}_4$ : 421.3331 [(M + H) $^+$ ], found: 421.3333 [(M + H) $^+$ ].

**Synthesis of 1,4,8,11-Tetraazabicyclo[6.6.3]heptadecane (3).** Intermediate **2** (3 g, 7.13 mmol) was dissolved in acetic acid (100 mL) in a 250 mL round-bottomed flask; 20%  $\text{Pd}(\text{OH})_2$  (1 g) was added to the solution. The resulting suspension was stirred under hydrogen gas at room temperature for 24 h. The reaction mixture was filtered through a diatomaceous earth pad, and the residue was washed with  $\text{CHCl}_3$  (3  $\times$  20 mL). The combined filtrate was evaporated under reduced pressure using a rotary evaporator, to give a clear oil. Diethyl ether addition to this oil afforded off-white solid **3** (1.7 g, 99% yield). TLC conditions: silica gel,  $\text{MeOH}/10\%$   $\text{NH}_4\text{OAc}$  1:1, Dragendorff's reagent,  $R_f$  value: 0.4–0.5. Spectroscopic data:  $^1\text{H}$  NMR (400 MHz,  $\text{CDCl}_3$ ):  $\delta$  3.62–3.18 (m, 8H), 3.16–2.76 (m, 12H), 2.09–1.87 (s, 4H), 1.86–1.75 (s, 2H); HR-MS (FAB) calculated for  $\text{C}_{13}\text{H}_{29}\text{N}_4$ : 241.2392 [(M + H) $^+$ ], found: 241.2397 [(M + H) $^+$ ].

**Synthesis of Diethyl ((1,4,8,11-tetraazabicyclo[6.6.3]heptadecan-4-yl)methyl)phosphonate (4).** Intermediate **3** (0.070 g, 0.29 mmol) was dissolved in anhydrous  $\text{CHCl}_3$  (30 mL) in a small round-bottomed flask. Triethyl phosphite (0.10 mL, 0.58 mmol) and paraformaldehyde (17.5 mg, 2 mol equiv of formaldehyde) were added to the solution. The resulting mixture was stirred at room temperature for 3–4 d. The reaction mixture was filtered through a diatomaceous earth bed, and the residue was washed with  $\text{CHCl}_3$  (3  $\times$  20 mL). The solvent was evaporated from the combined filtrate and washings under reduced pressure using a rotary evaporator. The resulting residue was purified by column chromatography, with silica gel as the stationary phase and  $\text{CH}_2\text{Cl}_2/\text{MeOH}$  (10:1.5) as the eluent, to afford transparent oil **4** (0.068 g, 60% yield). TLC conditions: silica gel,  $\text{CH}_2\text{Cl}_2/\text{MeOH}$  10:1.2, Dragendorff's reagent,  $R_f$  value: 0.5–0.6. Spectroscopic data:  $^1\text{H}$  NMR (400 MHz,  $\text{CDCl}_3$ ):  $\delta$  4.25–4.08 (m, 4H), 3.56–3.36 (m, 2H), 3.14–2.86 (m, 6H), 2.80–2.44 (m, 14H), 2.42–2.28 (bs, 1H), 1.97–1.82 (bs, 1H), 1.82–1.50 (m, 5H), 1.4–1.3 (t, 6H); electrospray ionization mass spectrometry (ESI-MS) calculated for  $\text{C}_{18}\text{H}_{40}\text{N}_4\text{O}_3\text{P}$ : 391.28 [(M + H) $^+$ ], found: 391.15 [(M + H) $^+$ ].

**Synthesis of tert-Butyl 2-(11-(diethoxyphosphoryl)methyl)-1,4,8,11-tetraazabicyclo[6.6.3]heptadecan-4-yl)acetate (5).** tert-Butyl bromoacetate (0.83 mL, 5.6 mmol) and anhydrous  $\text{K}_2\text{CO}_3$  (78 mg, 5.6 mmol) were added to a solution of **4** (1.1 g, 2.81 mmol) in anhydrous  $\text{CHCl}_3$  (80 mL) in a round-bottomed flask. The resulting mixture was stirred at room temperature for 3–4 d. The reaction mixture was filtered through a diatomaceous earth bed, which was washed with  $\text{CHCl}_3$  (3  $\times$  20 mL). The solvent from the combined filtrate and washings was evaporated under reduced pressure using a rotary evaporator. The resulting mixture was purified by column chromatography, with silica gel as the stationary phase and  $\text{CH}_2\text{Cl}_2/\text{MeOH}$  (10:2) as the eluent, to afford transparent oil **5** (1.28 g, 90% yield). TLC conditions: silica gel,  $\text{MeOH}/10\%$   $\text{NH}_4\text{OAc}$  1:1, Dragendorff's reagent,  $R_f$  value: 0.5–0.6. Spectroscopic data:  $^1\text{H}$  NMR (400 MHz,  $\text{CDCl}_3$ ):  $\delta$  4.22–4.08 (m, 4H), 3.76–2.28 (m, 24H), 2.2–1.6 (m, 6H), 2.80–2.44 (m, 14H), 1.55–1.4 (s, 9H), 1.4–1.3 (t, 6H);  $^{13}\text{C}$  NMR (125 MHz,  $\text{CDCl}_3$ ):  $\delta$  169.7, 81.7, 61.9, 56.8, 56.7, 56.2, 54.3, 53.5, 53.4, 52.1, 51.4, 51.2, 49.6, 48.3, 28.1, 23.7, 22.3, 19.9, 16.6; ESI-MS calculated for  $\text{C}_{24}\text{H}_{50}\text{N}_4\text{O}_5\text{P}$ : 505.35 [(M + H) $^+$ ], found: 505.21 [(M + H) $^+$ ].

**Synthesis of 2-(11-(Phosphonomethyl)-1,4,8,11-tetraazabicyclo[6.6.3]heptadecan-4-yl)acetic Acid Hydrochloride, PCB-TE1A1P (6).** PCB-TE1A1P precursor **5** (0.22 g, 0.43 mmol) was dissolved in 6 M HCl (30 mL) in a round-bottomed flask. The resulting solution was refluxed for 10 h. The solvent was removed

under reduced pressure using a rotary evaporator. The crude product was dried under vacuum overnight, dissolved in the minimum required volume of water, and purified using weakly acidic cation-exchange resin column chromatography. Amberlite CG50,  $\text{H}^+$  form resin was used, and the chromatographic column dimensions were 30 cm  $\times$  1 cm. The pure product was obtained by passing water through the column. Initially, excess acidic impurity was recovered, and the first 500 mL of aliquots were devoid of the desired product. Fractions containing the pure product were then obtained, as confirmed by TLC. All the fractions containing the product were combined, and the solvent was removed under reduced pressure using a rotary evaporator. Solvent traces were removed under direct vacuum to give the desired product as white solid **6** (0.14 g, 70% yield). TLC conditions: silica,  $\text{MeOH}/\text{NH}_4\text{OH}$  solution 10:1.2, or RP C-18,  $\text{MeOH}/10\%$   $\text{NH}_4\text{OAc}$  1:1, Dragendorff's reagent,  $R_f$  value: 0.6–0.7. Spectroscopic data:  $^1\text{H}$  NMR (500 MHz,  $\text{D}_2\text{O} + \text{MeOH}-d_4$ ):  $\delta$  3.58–2.70 (m, 24H), 2.22–1.84 (m, 6H);  $^{13}\text{C}$  NMR (125 MHz,  $\text{D}_2\text{O} + \text{MeOH}-d_4$ ):  $\delta$  174.7, 57.8, 57.2, 56.1, 54.5, 54.0, 53.6, 53.4, 52.8, 51.5, 49.7, 22.6, 21.3; HR-MS (FAB) calculated for  $\text{C}_{16}\text{H}_{34}\text{N}_4\text{O}_3\text{P}$ : 393.2267 [(M + H) $^+$ ], found: 393.2270 [(M + H) $^+$ ].

**Synthesis of Cu-PCB-TE1A1P.** The ligand PCB-TE1A1P (**6**) (134 mg, 0.31 mmol) and  $\text{Cu}(\text{ClO}_4)_2 \cdot 6\text{H}_2\text{O}$  (121 mg, 0.32 mmol) were dissolved in water (5 mL) in a small round-bottomed flask. The pH was adjusted to 8.5 with 1 M NaOH solution. The clear blue solution was heated at 100  $^\circ\text{C}$  for 10 min, cooled, and filtered through a diatomaceous earth bed. The filtrate solvent was evaporated under reduced pressure using a rotary evaporator, and the obtained blue solid was purified using semiprep HPLC (Nucleosil 100–7 C18 column 16  $\times$  250 mm and 7  $\mu\text{m}$ ; isocratic mobile phase consisting of water/MeOH (85:15), flow rate 4 mL/min). The purified fractions were combined, and the solvent was evaporated under reduced pressure using a rotary evaporator. The minimum necessary volume of MeOH was added, followed by diethyl ether diffusion. The deposited blue crystals were collected and dried (120.5 mg, 85% yield). HR-MS (FAB) calculated for  $\text{C}_{16}\text{H}_{32}\text{CuN}_4\text{O}_3\text{P}$ : 454.1406 [(M + H) $^+$ ], found: 454.1409 [(M + H) $^+$ ]. Visible electronic spectrum:  $\lambda_{\text{max}}$  (water) 629 nm. The purity of Cu-PCB-TE1A1P was checked using analytical HPLC (Waters Xbridge C-18 column, 4.6  $\times$  150 mm and 5  $\mu\text{m}$ ; mobile phase: 0.1% TFA-water/MeOH (94:6) and 1 mL/min isocratic flow rate).

**Spectrophotometric Acidic Decomplexation Studies of Cu-PCB-TE1A1P.** Cu-PCB-TE1A1P (2.72 mg, 3 mmol) in 5 M HCl (2 mL) was placed in a UV cuvette, and acidic decomplexation was examined at 90  $^\circ\text{C}$ , using a UV–vis spectrophotometer. The wavelength used was 629 nm ( $\lambda_{\text{max}}$ ). The decrease in the absorption maximum with time in a thermostated cell was used to monitor acidic decomplexation of the Cu complex. No decrease in absorbance was observed after reaction for 48 h, and the color of the reaction mixture was unchanged.

**High-Performance Liquid Chromatography Acidic Decomplexation Studies of Cu-PCB-TE1A1P.** Cu-PCB-TE1A1P (2.72 mg, 3 mmol) in 12 M HCl (2 mL) was placed in a Wheaton glass vial, and the solution was stirred at 90  $^\circ\text{C}$ . The HPLC profile of the Cu complex at various time intervals when subjected to 12 M HCl at 90  $^\circ\text{C}$  was observed. HPLC analysis was conducted at intervals of 0 min and 2, 4, 6, and 8 d. For HPLC analysis, an aliquot (70  $\mu\text{L}$ ) of the reaction mixture was transferred to a ship flask, and the solvent was evaporated under reduced pressure using a rotary evaporator, followed by addition of 70  $\mu\text{L}$  of water to the dried reaction mass. The obtained solution was vortexed carefully and transferred completely to a screw tube. A 20  $\mu\text{L}$  (27.2  $\mu\text{g}$ ) sample was taken from this stock solution and added to 80  $\mu\text{L}$  of water. This solution was injected into the HPLC system and analyzed. A reverse-phase Xbridge C-18 column (4.6  $\times$  150 mm, 5  $\mu\text{m}$ ) was used for HPLC analysis. Isocratic elution was performed using 0.1% TFA-water/MeOH (94:6) and a flow rate of 1 mL/min. When a Cu complex is demetalated in an acidic environment, reductions in the absorbance value in a specific UV region is seen. We took the UV–vis spectroscopic properties of the Cu-PCB-TE1A1P complex into account, and wavelengths of 280 and

629 nm ( $\lambda_{\text{max}}$ ) were used to monitor the reaction progress and acidic decomplexation of the complex.

**Electrochemical Studies of Cu-PCB-TE1A1P.** For cyclic voltammetry study of Cu-PCBTE1A1P, a working electrode of a glassy carbon with a 3 mm diameter and  $\Phi 3$  of 0.0707 cm<sup>2</sup> area was employed. The reference electrode was Ag/AgCl (saturated KCl), and the counter electrode was Pt wire. Cu-PCB-TE1A1P samples of concentration 3 mM were analyzed in 0.2 M phosphate buffer adjusted to pH 7.0 with glacial acetic acid. The scanning rate was 100 mV/s rate. Before performing the experiments, the Cu complex solutions were deoxygenated for a sufficient time with argon, and the scans were performed under argon.

**Radiolabeling of PCB-TE1A1P with <sup>64</sup>Cu.** PCB-TE1A1P chelator (1  $\mu\text{g}$ , 1  $\mu\text{L}$ ) in 0.1 M sodium acetate buffer (100  $\mu\text{L}$ , pH 8) was placed in a screw tube. Carrier-free <sup>64</sup>CuCl<sub>2</sub> (0.1–3.0 mCi) in 0.01 N HCl was added to this PCB-TE1A1P solution. The reaction mixture was incubated for 1 h at 60 °C. Formation of the desired <sup>64</sup>Cu-PCB-TE1A1P complex was monitored by radio-HPLC analysis using a reverse-phase Xbridge C-18 column (4.6  $\times$  150 mm, 5  $\mu\text{m}$ ). The mobile phase was 0.1% TFA–water/MeOH (94:6), with an isocratic flow rate of 1 mL/min. Radio-TLC was performed using a mobile phase consisting of MeOH/NH<sub>4</sub>OH solution (5:2) on silica plates.

**Radiolabeling of TE2A, TETA, and Cyclam with <sup>64</sup>Cu.** The stock solutions of the chelators (20  $\mu\text{g}/\mu\text{L}$ ) were first prepared in Milli-Q water. Complexation of the <sup>64</sup>Cu with TE2A, TETA, or cyclam was achieved by the addition of no-carrier added <sup>64</sup>CuCl<sub>2</sub> (100–300  $\mu\text{Ci}$ ) in 0.01 N HCl (1–2  $\mu\text{L}$ ) to a solution of the chelators (20  $\mu\text{g}$ ) in 100  $\mu\text{L}$  of 0.1 M ammonium acetate (pH 6.8) followed by incubation at 60 °C for 20 min. Formation of the corresponding <sup>64</sup>Cu complexes were confirmed by radio-TLC [C-18, MeOH/10% ammonium acetate (1:1)].

**Determination of Partition Coefficient of <sup>64</sup>Cu-PCB-TE1A1P.** The partition coefficient of <sup>64</sup>Cu-PCB-TE1A1P was determined as follows. The labeled complex (5  $\mu\text{L}$ , ~30–35  $\mu\text{Ci}$ ) was added to a mixture of 1-octanol (0.5 mL) and water (0.5 mL). The resulting solution was vigorously mixed, using a vortexer, for 5 min at room temperature to ensure proper contact between the solvents. The mixture was centrifuged for 5 min to ensure complete separation of the layers. Six experiments were performed. In each case, aliquots (0.1 mL) were removed from the water and octanol layers and placed in separate tubes, and their radioactivities were measured using a gamma counter. The radioactivity of the octanol layer was divided by that of the aqueous layer, and the negative logarithm of this quotient gave the partition coefficient. The average value of all readings was calculated to give the log(*P*) value.

**Measurement of Net Charge of <sup>64</sup>Cu-PCB-TE1A1P Using Electrophoresis.** The net charge of the <sup>64</sup>Cu complexes were determined by agarose gel electrophoresis. The 1.5% agarose gel was prepared in TAE buffer, and the comb was positioned at the center of gel instead of end. The labeled complexes were loaded in every alternate well, and the dye (DNA gel loading dye, Thermo scientific) was loaded at the terminal ends. Each <sup>64</sup>Cu complex (1  $\mu\text{Ci}$ ) was suspended in 5  $\mu\text{L}$  of deionized water. The gel was run at 50 V until the loading dye reached one-third of the gel. The electrophoresed gel was recorded with a fluorescent image analyzer (FLA-3000; FUJIFILM) and analyzed using software (Image reader FLA-3000; FUJIFILM).

**In Vitro Serum Stability of <sup>64</sup>Cu-PCB-TE1A1P.** <sup>64</sup>Cu-PCB-TE1A1P (50  $\mu\text{L}$ , 1 mCi) was added to fetal bovine serum (500  $\mu\text{L}$ ) in a screw tube, and the solution was gently stirred at 37 °C. Samples were removed at 0, 10, 30, and 60 min and 2, 4, 10, and 24 h after the radiocomplex was added to the serum. These aliquots were analyzed by radio-TLC using the conditions described above. The experiment was performed in duplicate.

**Stability Study by Measuring Copper Exchange Rate.** Copper exchange rate was measured in 0.005 M HEPES buffer (pH = 7.5) containing 0.01 M NaCl. Ligands (DOTA and PCB-TE1A1P) were prepared as a stock solution of 1000  $\mu\text{M}$  in Milli-Q water. Nonradioactive CuCl<sub>2</sub> solutions and radioactive <sup>64</sup>Cu solutions were also prepared as stock solutions of 100  $\mu\text{M}$  and 500  $\mu\text{Ci}/10 \mu\text{L}$ ,

respectively, in Milli-Q water. All solutions were prepared prior to the study.

Radiolabeling of the chelators with <sup>64</sup>Cu was done by adding no-carrier added <sup>64</sup>CuCl<sub>2</sub> (10  $\mu\text{L}$ , 500  $\mu\text{Ci}$ ) to the aqueous solution of the chelators (7.5  $\mu\text{L}$ ) and then incubating the mixture in HEPES buffer (982.5  $\mu\text{L}$ ) at 90 °C for 30 min. Formation of the corresponding <sup>64</sup>Cu complexes was confirmed by radio-TLC [C-18, MeOH/10% ammonium acetate (1:1) and silica, MeOH/10% ammonium acetate (5:2) for DOTA and PCB-TE1A1P, respectively].

Two different concentrations of nonradioactive copper (1 and 5  $\mu\text{M}$ ) were used to evaluate the stability of the <sup>64</sup>Cu complexes. For the stability study in 1  $\mu\text{M}$  CuCl<sub>2</sub> solution, to a solution of buffer (445  $\mu\text{L}$ ) and <sup>64</sup>Cu complexes (50  $\mu\text{L}$ ), CuCl<sub>2</sub> (5  $\mu\text{L}$ ) was added. The reaction mixture was then incubated at 37 °C up to 3 h using thermomixer (800 rpm), and per cent stability of both <sup>64</sup>Cu complexes was measured using radio TLC at 0, 30, 60, 120, and 180 min. For the stability study in 5  $\mu\text{M}$  CuCl<sub>2</sub> solution, to a solution of buffer (425  $\mu\text{L}$ ) and <sup>64</sup>Cu complexes (50  $\mu\text{L}$ ), CuCl<sub>2</sub> (25  $\mu\text{L}$ ) was added, and per cent stability was measured using radio TLC at the same time points. Final concentration of both chelators in both experiments was calculated to be 0.75  $\mu\text{M}$ . Two different TLC systems were used in this study. For <sup>64</sup>Cu-DOTA, C-18/MeOH/10% ammonium acetate (1:1) and for <sup>64</sup>Cu-PCB-TE1A1P, ITLC/50 mM EDTA were used as TLC system. In C-18/MeOH/10% ammonium acetate TLC condition, <sup>64</sup>Cu-DOTA and <sup>64</sup>Cu showed *R<sub>f</sub>* values of 0.94 and 0.0, respectively, whereas in ITLC/EDTA system <sup>64</sup>Cu-PCB-TE1A1P and <sup>64</sup>Cu showed *R<sub>f</sub>* values of 0.25 and 1.0, respectively. The per cent stability of the <sup>64</sup>Cu complexes was then plotted against time to obtain the kinetic stability graph of the corresponding <sup>64</sup>Cu complexes.

**Animal Models.** All animal experiments were conducted in compliance with the Animal Care and Use Committee requirements of Kyungpook National University.

**In Vivo Stability Study of <sup>64</sup>Cu-PCB-TE1A1P.** <sup>64</sup>Cu-PCB-TE1A1P of radioactivity 600  $\mu\text{Ci}$  in saline (200  $\mu\text{L}$ ) was injected into a six-week-old, male, Sprague–Dawley rat via the tail vein. After 1 h, the rat was sacrificed, and blood (3 mL) was collected in a heparinized tube. The blood was placed in microcentrifuge tubes and centrifuged at 13 200 rpm at 4 °C for 15 min. The supernatant from each tube was collected, and 400  $\mu\text{L}$  of solution was transferred to another tube. Ice-cold acetonitrile (400  $\mu\text{L}$ ) was added to this separated aliquot to precipitate proteins. This mixture was centrifuged at 13 200 rpm at 4 °C for 15 min; this was repeated to ensure complete separation of the layers. The supernatant was collected, and the liquid was evaporated under reduced pressure at 30 °C. The dried mass was diluted with water and analyzed by radio-HPLC using the same conditions as were used for <sup>64</sup>Cu-PCB-TE1A1P analysis. The HPLC fractions were collected at 0.25 min intervals, and their radioactivities were determined using a gamma counter. A graph of radioactivity versus time was plotted to monitor the in vivo stability of <sup>64</sup>Cu-PCB-TE1A1P.

**Biodistribution Study of <sup>64</sup>Cu-PCB-TE1A1P.** The body distribution and clearance of <sup>64</sup>Cu-PCB-TE1A1P was investigated using four-week-old, male, Sprague–Dawley rats (*n* = 5). <sup>64</sup>Cu-PCB-TE1A1P of radioactivity ~25  $\mu\text{Ci}$  in saline (200  $\mu\text{L}$ ) was injected into individual rats via the tail vein. Animals were sacrificed at 1, 4, and 24 h postinjection, according to the ethical guidelines. Various organs and tissues of interest, that is, blood, heart, lung, muscle, fat, bone, spleen, kidney, marrow, stomach, intestine, and liver, were removed and weighed, and their radioactivities were determined using a gamma counter. The data are reported in the percentage of injected dose per gram (% ID/g).

**Positron Emission Tomography Imaging Studies.** PET scans and image analyses were performed using a small-animal Inveon PET/CT scanner (Siemens). The imaging studies were performed on male BALB/c mice (*n* = 2). The mice were injected via the tail vein with <sup>64</sup>Cu-PCB-TE1A1P (~600  $\mu\text{Ci}$ ). At 1, 4, and 24 h after injection, the mice were anesthetized with isoflurane (1–2% in oxygen), positioned in the prone position, and scanned for 30 min and 1 and 2 h, respectively. The images were reconstructed using a two-dimensional



ordered-subsets expectation maximum algorithm, and no corrections were necessary for attenuation or scatter. PET images were quantified by region of interest analysis on the liver, kidney, muscle, and heart.

## ■ ASSOCIATED CONTENT

### Supporting Information

The Supporting Information is available free of charge on the ACS Publications website at DOI: 10.1021/acs.inorgchem.5b01386.

Synthesis of Cu-PCB-TE1A1P, HPLC spectra, spectrophotometric acidic decomplexation study, <sup>64</sup>Cu radiolabeling, serum stability, and biodistribution data of <sup>64</sup>Cu-PCB-TE1A1P. (PDF)

## ■ AUTHOR INFORMATION

### Corresponding Author

\*Fax: +82-53-426-4944. Phone: +82-53-420-4947. E-mail: yooj@knu.ac.kr.

### Author Contributions

#Equal contribution.

### Notes

The authors declare no competing financial interest.

## ■ ACKNOWLEDGMENTS

This work was supported by an R&D program through the National Research Foundation of Korea funded by the Ministry of Science, ICT & Future Planning (Nos. 2013R1A2A2A01012250, 2013M2A2A6042317, and 2012-0006386) and the Basic Research Laboratory Program (No. 2013R1A4A1069507). The Korea Basic Science Institute (Daegu) is acknowledged for providing assistance with NMR and MS measurements.

## ■ ABBREVIATIONS

- DTPA, diethylenetriaminepentaacetic acid  
 DOTA, 1,4,7,10-tetraazacyclododecane-*N,N',N'',N'''*-tetraacetic acid  
 TETA, 1,4,8,11-tetraazacyclotetradecane-*N,N',N'',N'''*-tetraacetic acid  
 NOTA, 1,4,7 triazacyclododecane-*N,N',N''*-triacetic acid  
 TE2A, 1,8-*N,N'*-bis(carboxymethyl)-1,4,8,11-tetraazacyclotetradecane  
 CB-TE2A, 4,11-bis(carboxymethyl)-1,4,8,11-tetraazabicyclo[6,6,2]hexadecane  
 PCB-TE2A, 4,11-bis(carboxymethyl)-1,4,8,11-tetraazabicyclo[6,6,3]hexadecane  
 CB-TE1A1P, 1,4,8,11-tetraazacyclotetradecane-1-(methanephosphonic acid)-8-(methanecarboxylic acid)  
 PCB-TE1A1P, 2-(11-(phosphonomethyl)-1,4,8,11-tetraazabicyclo[6.6.3]heptadecan-4-yl)acetic acid

## ■ REFERENCES

- Burke, B. P.; Archibald, S. J. *Annu. Rep. Prog. Chem., Sect. A: Inorg. Chem.* **2013**, *109*, 232–253.
- Abiraj, K.; Jaccard, H.; Kretzschmar, M.; Helm, L.; Maecke, H. R. *Chem. Commun.* **2008**, 3248–3250.
- Mansi, R.; Wang, X.; Forrer, F.; Kneifel, S.; Tamma, M.; Waser, B.; Cascato, R.; Reubi, J. C.; Maecke, H. R. *Clin. Cancer Res.* **2009**, *15* (16), 5240–5249.
- Gaynor, D.; Griffith, D. M. *Dalton Trans.* **2012**, *41*, 13239–13257.

- Cai, Z.; Anderson, C. J. *J. Labelled Compd. Radiopharm.* **2014**, *57*, 224–230.
- Wadas, T. J.; Anderson, C. J.; Wong, E. H.; Weisman, G. R. *Chem. Rev.* **2008**, *52*, 185–192.
- Shokeen, M.; Wadas, T. J. *Med. Chem.* **2011**, *7*, 413–429.
- Price, E. W.; Orvig, C. *Chem. Soc. Rev.* **2014**, *43*, 260–290.
- Ramogida, C. F.; Orvig, C. *Chem. Commun.* **2013**, *49*, 4720–4739.
- Bartholomä, M. D. *Inorg. Chim. Acta* **2012**, *389*, 36–51.
- Cooper, M. S.; Ma, M. T.; Sunassee, K.; Shaw, K. P.; Williams, J. D.; Paul, R. L.; Donnelly, P. S.; Blower, P. J. *Bioconjugate Chem.* **2012**, *23*, 1029–1039.
- Stasiuk, G. J.; Long, N. J. *Chem. Commun.* **2013**, *49*, 2732–2746.
- Anderson, C. J.; Dehdashti, F.; Cutler, P. D.; Schwarz, S. W.; Laforest, R.; Bass, L. A.; Lewis, J. S.; McCarthy, D. W. *J. Nucl. Med.* **2001**, *42*, 213–221.
- Prasanphanich, A. F.; Nanda, P. K.; Rold, T. L.; Ma, L.; Lewis, M. R.; Garrison, J. C.; Hoffman, T. J.; Sieckman, G. L.; Figueroa, S. D.; Smith, C. J. *Proc. Natl. Acad. Sci. U. S. A.* **2007**, *104*, 12462–12467.
- Pandya, D. N.; Kim, J. Y.; Park, J. C.; Lee, H.; Phapale, P. B.; Kwak, W.; Choi, T. H.; Cheon, G. J.; Yoon, Y. R.; Yoo, J. *Chem. Commun.* **2010**, *46*, 3517–3519.
- Pandya, D. N.; Bhatt, N.; Dale, A. V.; Kim, J. Y.; Lee, H.; Ha, Y. S.; Lee, J. E.; An, G. I.; Yoo, J. *Bioconjugate Chem.* **2013**, *24*, 1356–1366.
- Wadas, T. J.; Anderson, C. J. *Nat. Protoc.* **2007**, *1*, 3062–3068.
- Pandya, D. N.; Dale, A. V.; Kim, J. Y.; Lee, H.; Ha, Y. S.; An, G. I.; Yoo, J. *Bioconjugate Chem.* **2012**, *23*, 330–335.
- Pandya, D. N.; Bhatt, N.; An, G. I.; Ha, Y. S.; Soni, N.; Lee, H.; Lee, Y. J.; Kim, J. Y.; Lee, W.; Ahn, H.; Yoo, J. *J. Med. Chem.* **2014**, *57*, 7234–7243.
- Ferdani, R.; Stigers, D. J.; Fiamengo, A. L.; Wei, L.; Li, B. T.; Golen, J. A.; Rheingold, A. L.; Weisman, G. R.; Wong, E. H.; Anderson, C. J. *Dalton Trans.* **2012**, *41*, 1938–1950.
- Zeng, D.; Ouyang, Q.; Cai, Z.; Xie, X. Q.; Anderson, C. J. *Chem. Commun.* **2014**, *50*, 43–45.
- Lewis, M. R.; Boswell, A.; Laforest, R.; Buettner, T. L.; Ye, D.; Connett, J. M.; Anderson, C. J. *Cancer Biother. Radiopharm.* **2001**, *16*, 483–494.
- Smith-Jones, P. M.; Fridrich, R.; Kaden, T. A.; Novak-Hofer, I.; Siebold, K.; Tschudin, D.; Maecke, H. R. *Bioconjugate Chem.* **1991**, *2*, 415–421.
- Parker, D. *Chem. Soc. Rev.* **1990**, *19*, 271–291.
- Cox, J. P. L.; Craig, A. S.; Helps, I. M.; Jankowski, K. J.; Parker, D.; Eaton, M. A. W.; Millican, A. T.; Millar, K.; Beeley, N. R. A.; Boyce, B. A. *J. Chem. Soc., Perkin Trans. 1* **1990**, 2567–2576.
- Bass, L. A.; Wang, M.; Welch, M. J.; Anderson, C. J. *Bioconjugate Chem.* **2000**, *11*, 527–532.
- Boswell, C. A.; Sun, X.; Niu, W.; Weisman, G. R.; Wong, E. H.; Rheingold, A. L.; Anderson, C. J. *J. Med. Chem.* **2004**, *47*, 1465–1474.
- Di Bartolo, N. M.; Sargeson, A. M.; Donlevy, T. M.; Smith, S. V. *J. Chem. Soc., Dalton Trans.* **2001**, 2303–2309.
- Ferreira, C. L.; Yapp, D. T.; Lamsa, E.; Gleave, M.; Bensimon, C.; Jurek, P.; Kiefer, G. E. *Nucl. Med. Biol.* **2008**, *35*, 875–882.
- Boros, E.; Rybak-Akimova, E.; Holland, J. P.; Rietz, T.; Rotile, N.; Blasi, F.; Day, H.; Latifi, R.; Caravan, P. *Mol. Pharmaceutics* **2014**, *11* (2), 617–629.
- Royal, G.; Dahaoui-Gindre, V.; Dahaoui, S.; Tabard, A.; Guillard, R.; Pullumbi, P.; Lecomte, C. *Eur. J. Org. Chem.* **1998**, *1998*, 1971–1975.
- Woodin, K. S.; Heroux, K. J.; Boswell, C. A.; Wong, E. H.; Weisman, G. R.; Tomellini, S. A.; Anderson, C. J.; Zakharov, L. N.; Rheingold, A. L. *Eur. J. Inorg. Chem.* **2005**, *2005*, 4829–4833.
- Dale, A. V.; Pandya, D. N.; Kim, J. Y.; Lee, H.; Ha, Y. S.; Bhatt, N.; Kim, J.; Seo, J. J.; Lee, W.; Kim, S. H.; Yoon, Y.-R.; An, G. I.; Yoo, J. *ACS Med. Chem. Lett.* **2013**, *4*, 927–931.
- Maheshwari, V.; Dearling, J. L. J.; Treves, S. T.; Packard, A. B. *Inorg. Chim. Acta* **2012**, *393*, 318–323.

- (35) Juran, S.; Walther, M.; Stephan, H.; Bergmann, R.; Steinbach, J.; Kraus, W.; Emmerling, F.; Comba, P. *Bioconjugate Chem.* **2009**, *20*, 347–359.
- (36) Ferreira, C. L.; Holley, I.; Bensimon, C.; Jurek, P.; Kiefer, G. E. *Mol. Pharmaceutics* **2012**, *9*, 2180–2186.
- (37) Sun, X.; Wuest, M.; Kovacs, Z.; Sherry, A. D.; Motekaitis, R.; Wang, Z.; Martell, A. E.; Welch, M. J.; Anderson, C. J. *JBIC, J. Biol. Inorg. Chem.* **2003**, *8*, 217–225.
- (38) Tanwar, J.; Datta, A.; Tiwari, A. K.; Thirumal, M.; Chuttani, K.; Mishra, A. K. *Bioconjugate Chem.* **2011**, *22*, 244–255.
- (39) Gano, L.; Marques, F.; Campello, M. P.; Balbina, M.; Lacerda, S.; Santos, I. Q. *J. Nucl. Med. Mol. Imaging* **2007**, *51*, 6–15.
- (40) Vitha, T.; Kubicek, V.; Hermann, P.; Elst, L. V.; Muller, R. N.; Kolar, Z. I.; Wolterbeek, H. T.; Breeman, W. A. P.; Lukes, I.; Peters, J. A. *J. Med. Chem.* **2008**, *51*, 677–683.
- (41) Forsterova, M.; Jandurova, Z.; Marques, F.; Gano, L.; Lubal, P.; Vanek, J.; Hermann, P.; Santos, I. *J. Inorg. Biochem.* **2008**, *102*, 1531–1540.
- (42) Yoo, J.; Reichert, D. E.; Welch, M. J. *J. Med. Chem.* **2004**, *47*, 6625–6637.
- (43) Sprague, J. E.; Peng, Y.; Sun, X.; Weisman, G. R.; Wong, E. H.; Achilefu, S.; Anderson, C. J. *Clin. Cancer Res.* **2004**, *10*, 8674–8682.